9th Asia-Pacific Conference on Plasma Physics, 21-26 Sep, 2025 at Fukuoka

Comprehensive Diagnosis of Laser-Plasma Interaction in Capillary Waveguides for High-Harmonic Generation

Shih-Chi Kao[1], Kai-Xiang Li[1], Jia-Wen Gu[1], Jian-He Lin[1], and Hsu-Hsin Chu[1]
[1] Department of Physics, National Central University, Taiwan.
blackdiamondkao@gmail.com

Gas-filled capillary waveguides are widely used in laser-plasma interaction applications to extend the interaction length, enabling ionization-induced self-compression [1], high-harmonic generation (HHG) [2], laser wakefield electron acceleration [3], and more. In this work, we focus on HHG in argon-filled capillary waveguides. Plasma formation inside the capillary modifies the guiding properties and influences the HHG phase-matching conditions [4,5]. Direct plasma diagnostics in such systems are rare, with most studies focusing on discharge plasmas [6]. Here, we employ frequency-domain interferometry (FDI) to probe the plasma produced by near-IR femtosecond laser pulses [7], enabling detailed characterization of plasma density evolution and optimization of the HHG phase matching conditions under highly ionized states.

Five diagnostic tools were employed. An FDI was implemented to measure the plasma density inside the gas-filled capillary. A relay-imaging system captured the input and output beam profiles of the driving laser pulse, while an energy meter and a spectrometer monitored its attenuation and spectral modulation. Finally, a home-made EUV spectrometer characterized the HHG output. Using the information gathered from all these tools, the complete HHG phase-matching condition arising from plasma dispersion, waveguide dispersion, and HHG dipole phase variation was resolved.

The high-power Ti:sapphire laser system we built at National Central University was used to provide 810-nm, 40-fs laser pulses for driving HHG [8]. The driving laser beam was focused into an 8-mm-long, 200-μm-diameter fused-silica capillary by an off-axis parabolic mirror. The capillary was mounted in a cell, with two transverse holes drilled near both ends for gas injection. The injection was controlled by a pulsed valve. First, we used the FDI to measure the plasma density produced by the driving pulse at different backing pressures of the pulse valve. The results are shown in Fig. 1, which clearly indicate that the plasma density increases monotonically as the backing pressure increases. Furthermore, we found that when the plasma density exceeded the critical value (7×10^{16} cm^{-3})[9], the driving beam profile was significantly modified, as shown in Fig. 2. It was coupled from the original EH11 mode to the EH12 mode due to ionization-induced defocusing.

Finally, after optimization, we obtained the HHG output with the shortest wavelength of 17 nm, corresponding to a photon energy of 73 eV (Fig.3). This exceeds the traditional cutoff photon energy of 63.7 eV for HHG from argon atoms, indicating that phase-matching condition was achieved under our highly ionized state.

Our analysis revealed that the attenuation of the driving laser pulse (attenuation coefficient = 0.007 mm^{-1}) induced a positive dipole phase variation, which compensated for the negative plasma dispersion and waveguide dispersion. Consequently, the phase-matching condition can be extended to higher photon energies. We believe that HHG from plasmas offers a promising approach for generating efficient EUV/x-ray sources.

References

[1] S.A. Skobelev et al., JETP Lett. 89, 540 (2009).
[2] Y.-L. Liu et al., Opt. Express 30, 1365 (2022).
[3] N.E. Andreev et al., IEEE Trans. Plasma Sci. 36, 1746 (2008).
[4] J.R. Davies and J.T. Mendonça, Phys. Rev. E 62, 7168 (2000).
[5] Q. Ran et al., IEEE Photon. Technol. Lett. 32, 1393 (2020).
[6] J. Daniels et al., Phys. Plasmas 22, 073112 (2015).
[7] E. Tokunaga et al., J. Opt. Soc. Am. B 12, 753 (1995).
[8] Y.-L. Liu et al., Opt. Express 32, 40620 (2024).
[9] G. Tempea and T. Brabec, Opt. Lett. 23, 1286 (1998).

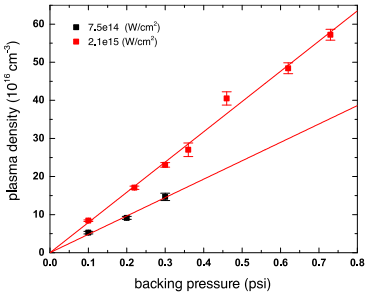

Figure 1: Plasma density versus backing pressure

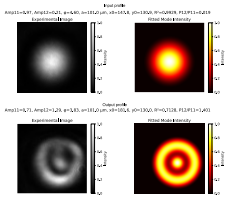

Figure 2: Mode transition from EH11 to EH12

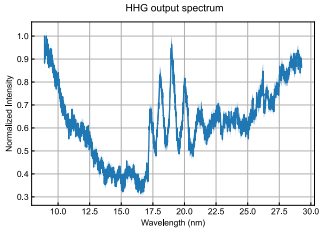

Figure 3: HHG spectrum